

The Ly α /H β intensity ratio in the spectra of QSOs

Jack A. Baldwin[★] *Lick Observatory, Board of Studies in Astronomy and Astrophysics, University of California, Santa Cruz*

Received 1976 December 16

Summary. The average Ly α /H β intensity ratio in the spectra of QSOs is found to be much smaller than expected. The continuum energy distributions of some QSOs are shown to be modestly reddened, but it is probable that the main cause of the small Ly α /H β ratio is enhancement of H β rather than the depletion of Ly α .

1 Introduction

The relative intensities of Ly α and H β in the spectra of QSOs are of considerable interest, both because of the possible use of these two lines in linking together the spectra of high- and low-redshift QSOs and because of the information that their relative strengths can convey about physical conditions in and near the ionized gas. The ratio expected in a pure recombination spectrum is at least 22 (Miller 1974). Several authors (Davidson 1972; MacAlpine 1972; Weedman 1976) have adopted $I(\text{Ly}\alpha)/I(\text{H}\beta) = 40$, assuming that we are seeing a spectrum which is basically due to recombinations but which is augmented by collisionally excited Ly α emission. Wampler (1968) had made a preliminary observational estimate that placed this ratio somewhere between 7 and 200. A more recent observational determination based on equivalent widths estimated from the photographic spectra of a large number of QSOs suggests that $I(\text{Ly}\alpha)/I(\text{H}\beta) \approx 18$ (Chan & Burbidge 1975). By combining spectrophotometric data for 26 QSOs, we will show here that this ratio is in all probability as small as $I(\text{Ly}\alpha)/I(\text{H}\beta) \approx 3$. We will also show that the continuous spectra of at least two of these QSOs are modestly reddened, but that the average Ly α equivalent width indicates that it is unlikely that Ly α has been strongly attenuated by reddening or by any other means.

2 The Ly α /H β ratio

The rest wavelengths of Ly α and H β are too far apart for both of these lines to be observable in the optical spectrum of any single QSO. The average equivalent widths of these lines in the spectra of QSOs of different redshifts provide one estimate of their relative intensities. Ly α is normally blended with N v λ 1240 which contributes around one fourth of the

[★] Present address: University of Cambridge, Institute of Astronomy, Madingley Road, Cambridge CB3 0HA.

total intensity. Table 1 lists average equivalent widths for $\text{Ly}\alpha + \text{N V}$ and $\text{H}\beta$, reduced to the rest frame, from several photometric studies. Assuming that the properties of QSOs at different redshifts are on average the same and that the spectra may be characterized by a power-law of the form $f_\nu \propto \nu^{-\alpha}$, we have $I(\text{Ly}\alpha)/I(\text{H}\beta) = (4861/1216)^{2-\alpha} W_\lambda(\text{Ly}\alpha)/W_\lambda(\text{H}\beta)$. Using the final averages from Table 1 (with $W_\lambda(\text{Ly}\alpha) = 0.75 W_\lambda(\text{Ly}\alpha + \text{N V})$) and taking as typical value $\alpha = 1$, we find $I(\text{Ly}\alpha)/I(\text{H}\beta) = 2.3$. This is much smaller than the ratio expected for a recombination spectrum, and our average equivalent widths $W_\lambda(\text{Ly}\alpha) = 54 \text{ \AA}$ and $W_\lambda(\text{H}\beta) = 92 \text{ \AA}$ differ considerably from the values 230 and 52 \AA found by Chan & Burbidge (1975). Based on the level of agreement between different samples in Table 1, the average equivalent widths found here are probably accurate to about 25 per cent.

Table 1. Average equivalent widths.

Number of QSOs	$W_\lambda(\text{Ly}\alpha + \text{N V})$ (\AA , rest frame)	$W_\lambda(\text{H}\beta)$ (\AA , rest frame)	Source
13	—	100	Baldwin (1975)
1	—	66	Measured from data of Wampler <i>et al.</i> (1975)
6	—	78	This paper
14	70	—	Baldwin (1977)
9	76	—	Osmer & Smith (1976)

Final average (all QSOs equally weighted):

72 92

Another estimate of the $\text{Ly}\alpha/\text{H}\beta$ ratio, one which does not depend on an assumed continuum shape, can be obtained by piecing together a composite spectrum based on the relative intensities of several of the stronger emission lines. Table 2 lists what we believe to be reasonably accurate relative intensities for the $\text{Ly}\alpha \lambda 1216 + \text{N V } \lambda 1240$, $\text{C IV } \lambda 1549$, $\text{C III } \lambda 1909$, $\text{Mg II } \lambda 2800$ and $\text{H}\beta \lambda 4861$ lines in a number of QSO spectra. These spectra cover at least the range $\text{Ly}\alpha$ — C III , C III — Mg II , or Mg II — $\text{H}\beta$. Also listed are continuum fluxes for most objects, either measured at or extrapolated to a rest wavelength of 2650 \AA in each spectrum, and continuum luminosities worked out for both $q_0 = 0$ and $q_0 = +1$ following the formulae given by Oke, Neugebauer & Becklin (1970) but adjusted to $H_0 = 50$. In addition, Table 2 lists for each object an approximate value of α , the continuum slope. The letter *c* appended to the slope indicates that the continuum is markedly curved and cannot be adequately fitted by any single power law.

The first composite spectrum listed at the bottom of Table 2 was computed using all of the listed QSOs, by finding the average line strengths relative to either $\text{Ly}\alpha$ or Mg II and then renormalizing the average C III , Mg II and $\text{H}\beta$ strengths in the low-redshift objects so that the C III strength would be the same as for the high-redshift objects. Very similar answers were obtained when the renormalization was made on the basis of $I(\text{C IV})$ rather than $I(\text{C III})$. In order to see if the effects of different average luminosities or different average continuum slopes among objects of different redshifts might have influenced these results, separate composite spectra were worked out for subgroups of QSOs which have similar continuum luminosities or continuum slopes. These results are also listed at the end of Table 2 and are not markedly different from the composite spectrum for all objects. In all cases we find $3 \leq I(\text{Ly}\alpha + \text{N V})/I(\text{H}\beta) \leq 6$. Again taking $I(\text{Ly}\alpha) = 0.75 I(\text{Ly}\alpha + \text{N V})$, our final estimate is $I(\text{Ly}\alpha)/I(\text{H}\beta) \approx 3$.

3 Discussion

The presence of the powerful continuum sources in QSOs suggests that photoionizations are the dominant form of energy input into the gas and that we are seeing a modified recombination spectrum. One possible explanation of the small Ly α /H β ratio is that Ly α is attenuated, and reddening by dust is a quite plausible mechanism for this attenuation. We have examined the continuous energy distributions of 20 QSOs (Fig. 1) for evidence of reddening. The ultraviolet extinction curve (Savage 1975; Nandy *et al.* 1975; Bless & Savage 1972) is characterized by a broad absorption feature near 2175 Å and (usually) by a general flattening in the range 1300–2200 Å. Fig. 1 shows that these features are mirrored in the spectra of PHL 938 and Ton 490, and that there is some suggestion of the λ 2175 feature in the spectra of 3C 286 and CTA 102. Beneath the spectrum of PHL 938 we have plotted the spectrum of a power-law with $\alpha=0.7$ which has been reddened by the ‘average’ uv extinction curve of Bless & Savage (1972) by an amount corresponding to $E(B-V)=0.08$. A similar curve for Ton 490 with $\alpha=1.1$ and $E(B-V)=0.04$ is also shown on Fig. 1. These curves are quite good fits, especially given the variability in the extinction curve near Ly α (Bless & Savage 1972), and in our opinion demonstrate that the continua of PHL 938 and Ton 490 are reddened. But most of the other QSOs shown on Fig. 1 do not have the absorption dip or marked change in continuum slope near λ 2175, and we tentatively conclude that these

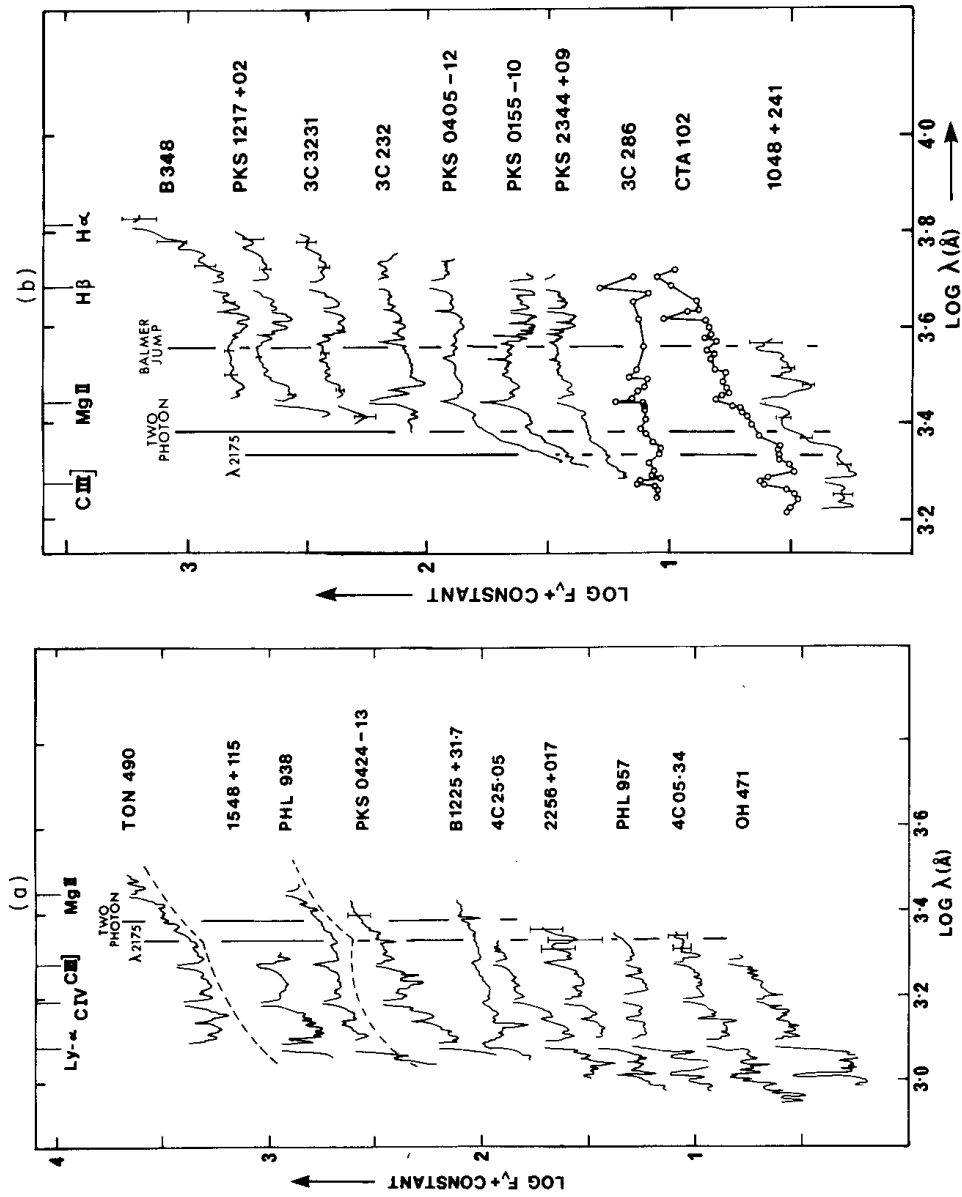


Figure 1. (a), (b) Smoothed, schematic continuum energy distributions for twenty QSOs, taken from the references cited in Table 2. Observed flux is plotted against the rest wavelengths. Error bars indicate range of scatter between adjacent data points, where it is large. The line marked ‘two photon’ indicates the expected position of the maximum two-photon emission.

Object	Ref.*	z	α	$\log f_{\nu}^{\dagger}$	$\log L_{\nu}^{\dagger}$ ($q_0 = +1$)	$\log L_{\nu}^{\dagger}$ ($q_0 = 0$)	I(Ly α +NV)	I(CIV)	I(CIII)	I(Mg II)	I(H β)
3C 273	1	0.158	0.5	(-24.55)	31.41	31.48			100:	139	
B340	2	0.184	2.6	(-26.28)	29.81	29.88			100	71	
PKS 1217+02	2	0.240	0.8	(-26.12)	30.18	30.28			100	108	
3C 323.1	2	0.264	0.9	(-26.13)	30.24	30.35			100	100	
PHL 1186	2	0.269	1.5	(-26.34)	30.05	30.16			100	91	
3C 232	3	0.529	0.7	-26.01	30.88	31.09			100	17	
PKS 0405-12	3	0.575	0.5	-25.47	31.48	31.70			100	121:	
PKS 0155-10	3	0.616	0.5 \dagger	-26.44	30.56	30.79			100	89	
PKS 2344+09	3	0.677	1.3	-26.00	31.07	31.32		46	100	81	
3C 286	4	0.848	0.2	-26.30	30.92	31.23			100	130	
CTA 102	4	1.04	0.9	-26.37	30.98	31.35			100	96	
1048+241	3	1.27	1.1 \dagger	-27.27	30.21	30.64			100	43	
2328+107	5	1.50	1.0:						100	90	
1511+103	5	1.55	1.1:						100	63	
Ton 490	6	1.63	1.0 \dagger	-26.09	31.54	32.06		200	100	89	
1548+115b	6	1.90	0.6	(-26.80:)	30.93	31.51			100	24	
4C 29.50	6	1.92	2.0 \dagger	(-27.30:)	30.43	31.02			100	13	
PHL 938	6	1.95	0.9 \dagger	-26.17	31.57	32.16			100	120	
1559+173	5	1.96	0.3:						240	19	
PKS 0424-13	6	2.16	1.5	-26.52	31.28	31.92			33	70	
B1225+31.7	6	2.23	0.6 \dagger	-25.71	32.11	32.76			100	40	

Table 2. Relative emission-line intensities.

4C 23.03	0	2.34	1.0	(-20.11)	31.01	31.75	100	50	26	27	28	24	30	24	23	16	33
2256+017	6	2.66	1.0	(-26.90)	31.02	31.75	100	46	14	26	25	30	30	26	30	16	33
PHL 957	6	2.69	0.6	(-26.00)	31.92	32.66	100	28	30	27	28	24	30	26	30	16	33
4C 05.34	6	2.86	1.2	(-26.46)	31.50	32.27	100	33	13	26	28	24	30	26	30	16	33
OH 471	6, 7	3.39	1.6	-26.66	31.39	32.25	100	31	20	26	28	24	30	26	30	16	33
Composite spectra:																	
All Objects																	
$\alpha < 1$																	
$\alpha \geq 1$																	
$q_0 = +1$:																	
30.1 < log L < 30.6	100	56	13	30	30	30	100	45	26	27	28	24	30	26	30	16	33
30.6 < log L < 31.1	100	46	21	23	30	24	100	39	36	26	28	24	30	26	30	16	33
31.1 < log L < 31.6	100	47	19	20	30	24	100	49	20	26	28	24	30	26	30	16	33
$q_0 = 0$:																	
30.6 < log L < 31.1	100	56	13	30	30	30	100	45	26	27	28	24	30	26	30	16	33
31.1 < log L < 31.8	100	46	21	23	30	24	100	39	36	26	28	24	30	26	30	16	33

Notes:

Entries followed by colons have estimated uncertainties \pm 50 per cent.* References: (1) – equivalent width from Baldwin (1975) and continuum observations of Oke & Shields (1976); (2) – Baldwin (1975); (3) – this paper; (4) – Oke, Neugebauer & Becklin (1970); (5) – Smith *et al.* (1977); (6) – Baldwin (1977); (7) – Oke (1974).† Measured at λ 2650 in rest frame. Flux in $\text{erg cm}^{-2} \text{s}^{-1} \text{Hz}^{-1}$, with extrapolated values in parentheses. Luminosity in $\text{erg s}^{-1} \text{Hz}^{-1}$.

objects are *not* appreciably reddened. McKee & Petrosian (1974) have discussed some of the implications of the presence or absence of reddening in QSO spectra.

The observed $\text{Ly}\alpha/\text{H}\beta$ ratio is at least eight times smaller than is expected from a recombination spectrum. If this is the result of reddening, then according to Bless & Savage's (1972) average extinction curve this corresponds to $E(B-V) \approx 0.35$. This is greater than the largest amount of observed reddening of the continuum, and much greater than the average amount, so the line-emitting gas would have to be considerably more heavily reddened than the continuum. This would be plausible only if the gas (and along with it the dust) is concentrated in clouds or a disk and typically does not obscure the continuum source, as is suggested by other considerations discussed below. The required $E(B-V) \approx 0.35$ is also in reasonable agreement with the average $E(B-V) = 0.5$ which can be inferred for low-redshift QSOs on the assumption that the observed Balmer decrements represent a reddened recombination spectrum (Baldwin 1975), but the $\text{H}\beta/\text{P}\alpha$ intensity ratio in the spectrum of 3C273 apparently rules out reddening as the cause of the steep Balmer decrement in at least that object (Grasdalen 1976). The evidence for heavy reddening is therefore at best ambiguous.

$\text{Ly}\alpha$ photons could also be destroyed if they were severely trapped inside optically thick gas clouds, where they could then be selectively depleted either by absorption on dust grains, by photoionizations from the $n=2$ level, or by conversion to the two-photon continuum. The spectra in Fig. 1 show no evidence for two-photon emission, which would appear as a broad hump starting at the position of $\text{Ly}\alpha$ and peaking at $\lambda 2431$. The prominent hump in the spectrum of 1048 + 241 is too sharply peaked and the maximum occurs at too large a wavelength to be the two-photon continuum. Using relations given by Spitzer & Greenstein (1951) we can find a limit on the number of photons in the two-photon continuum in terms of the maximum deviation of any of the other spectra from a power-law shape, and when compared to the number of photons in a $\text{Ly}\alpha$ line of average equivalent width this gives as a limit the ratio (number converted to two-photon)/(number left in $\text{Ly}\alpha$) ≤ 2 . Thus, two-photon emission could account for no more than one fourth of the missing $\text{Ly}\alpha$ photons and still remain undetected. The other two processes for the selective destruction of $\text{Ly}\alpha$ could easily be more effective than two-photon conversion, but we cannot place similar observational limits on their importance.

In any of these cases in which $\text{Ly}\alpha$ photons are depleted while the continuum radiation is left unaffected, the equivalent width of $\text{Ly}\alpha$ will also have been decreased by at least a factor of eight. In the photoionization model, if the ionized gas is in a shell which completely covers the continuum source and is extremely optically thick so that hydrogen can absorb all of the photons between 912 Å and the He II Lyman continuum edge at 228 Å, we expect the $\text{Ly}\alpha$ equivalent widths to be $W_\lambda(\text{Ly}\alpha) = 680$ Å for a continuum slope $\alpha = 1$ and 1680 Å for $\alpha = 0$. But the general absence of Lyman continuum absorption in the emission-line redshift system of any high-redshift QSO (Oke 1974; Baldwin *et al.* 1976) implies that only a small proportion (probably ≤ 0.1) of the continuum radiation could be intercepted by optically thick gas clouds. Decreasing the predicted equivalent widths by this factor of 10 brings them into reasonable agreement with the observed equivalent widths ($W_\lambda(\text{Ly}\alpha) = 54$ only if $\text{Ly}\alpha$ has *not* been attenuated).

These considerations suggest that instead $\text{H}\beta$ has been enhanced by a large factor. The observed Balmer decrements in low-redshift QSOs indicate that $\text{H}\beta$ cannot have been strengthened by more than a factor of two as a result of collisional excitations from the ground state (Baldwin 1975) or from the $n=2$ level (Netzer 1976) in simple models. Perhaps the combination of high gas and radiation densities can lead to some more subtle means of increasing the population of the higher levels, possibly in a situation where the timescale for upwards transitions becomes as short as the de-excitation timescale.

Other possibilities are that these lines are not formed by recombinations or that any composite QSO spectrum is made meaningless by basic differences between QSOs of different redshifts. The best way to avoid the latter uncertainty is to obtain simultaneous rocket uv and optical measurements of the Ly α and H β strengths in the spectra of low-redshift QSOs and Type I Seyfert galaxies.

Acknowledgments

I thank Cyril Hazard, Martin Rees and John Whelan for some very helpful suggestions. This research was partially supported by NSF Grant GP 29684 and also by the Science Research Council.

References

- Baldwin, J. A., 1975. *Astrophys. J.*, **201**, 26.
 Baldwin, J. A., 1977. *Astrophys. J.*, in press.
 Baldwin, J. A., Smith, H. E., Burbidge, E. M., Hazard, C., Murdoch, H. S. & Jauncey, D. L., 1976. *Astrophys. J.*, **206**, L83.
 Bless, R. C. & Savage, B. D., 1972. *Astrophys. J.*, **171**, 293.
 Chan, Y-W. T. & Burbidge, E. M., 1975. *Astrophys. J.*, **198**, 45.
 Davidson, K., 1972. *Astrophys. J.*, **171**, 213.
 De Veny, J. B., Osborn, W. H. & Janes, K., 1971. *Publ. astr. Soc. Pacific*, **83**, 611.
 Grasdalen, G. L., 1976. *Astrophys. J.*, **208**, L11.
 Hazard, C., Jauncey, D. L., Sargent, W. L. W., Baldwin, J. A. & Wampler, E. J., 1973. *Nature*, **246**, 205.
 MacAlpine, G. M., 1972. *Astrophys. J.*, **175**, 11.
 Miller, J. S., 1974. *A. Rev. Astr. Astrophys.*, **12**, 331.
 McKee, C. F. & Petrosian, V., 1974. *Astrophys. J.*, **189**, 17.
 Nandy, K., Thompson, G. I., Jamar, C., Monfils, A. & Wilson, R., 1975. *Astr. Astrophys.*, **44**, 195.
 Netzer, H., 1976. Preprint.
 Oke, J. B., 1974. *Astrophys. J.*, **189**, L47.
 Oke, J. B., Neugebauer, G. & Becklin, E. E., 1970. *Astrophys. J.*, **159**, 341.
 Oke, J. B. & Shields, G. A., 1976. *Astrophys. J.*, **207**, 713.
 Osmer, P. S. & Smith, M. G., 1976. Preprint.
 Robinson, L. B. & Wampler, E. J., 1972. *Publ. astr. Soc. Pacific*, **84**, 161.
 Savage, B. D., 1975. *Astrophys. J.*, **199**, 92.
 Smith, H. E., Burbidge, E. M., Baldwin, J. A., Tohline, J., Wampler, E. J., Hazard, C. & Murdoch, H. S., 1977. *Astrophys. J.*, in press.
 Spitzer, L. & Greenstein, J. L., 1951. *Astrophys. J.*, **141**, 407.
 Wampler, E. J., 1968. *Astrophys. J.*, **153**, 19.
 Wampler, E. J., Robinson, L. B., Burbidge, E. M. & Baldwin, J. A., 1975. *Astrophys. J.*, **198**, L49.
 Weedman, D. W., 1976. *Astrophys. J.*, **208**, 30.

Appendix

New observational material

Table 3 lists some details concerning the observations of seven of the objects for which data appear in Tables 1 and 2. These observations were made with the Image Tube Scanner (Robinson & Wampler 1972) at the Lick Observatory 3-m telescope using resolutions of about 7 and 15 Å. The continuum energy distributions of 3C232, PKS0405–12, PKS0155–10 and PKS2344+09 were carefully measured using large (6×6 arcsec) entrance apertures; the other spectra are somewhat less well calibrated. Table 2 lists relative emission line strengths for these objects, as well as previously unpublished line strengths for a number of higher redshift QSOs observed by Baldwin (1977).

E

Table 3. New observational material.

Object	z	$W_{\lambda}(\text{Mg II})$ (\AA , rest frame)	$W_{\lambda}(\text{H}\beta)$ (\AA , rest frame)	Observed wavelength range (\AA)	Dates observed
PHL 658	0.450	100:	100:	5815–7565	1974 Oct 22
PKS 1327–21	0.528	55	120	3100–7994	1976 Jan 29 and Mar 26
3C 232	0.529	63	21	3548–8700	1974 Oct 21; 1975 Jan 13
PKS 0405–12	0.575	23	70:*	3100–8700	1974 Oct 21 and Nov 11; 1975 Jan 12
PKS 0155–10	0.616	30	87	3100–8450	1974 Oct 22 and Nov 11; 1975 Aug 7, Aug 8, Aug 9 and Aug 10
PKS 2344+09	0.677	37	75	3100–8700	1974 Aug 27, Aug 28, Oct 21, Nov 11 and Dec 17
1048+241	1.27	83		3592–8700	1975 Jan 12, Aug 7, Aug 8 and Aug 9 1976 Jan 29

Notes:

Entries followed by colons have estimated uncertainties ± 50 per cent.All objects are from De Veny, Osborn & Janes (1971) catalogue, except 1048+241 is from Hazard *et al.* (1973).* H β is confused with the atmospheric A band absorption in the spectrum of PKS 0405–12.